

The Anomalous Acceleration of PSR J2043+1711: Long-Period Orbital Companion or Stellar Flyby?

THOMAS DONLON II,¹ SUKANYA CHAKRABARTI,¹ MICHAEL T. LAM,^{2,3,4} DANIEL HUBER,^{5,6} DANIEL HEY,⁵
ENRICO RAMIREZ-RUIZ,⁷ BENJAMIN SHAPPEE,⁵ DAVID L. KAPLAN,⁸ GABRIELLA AGAZIE,⁸ AKASH ANUMARLAPUDI,⁸
ANNE M. ARCHIBALD,⁹ ZAVEN ARZOUMANIAN,¹⁰ PAUL T. BAKER,¹¹ PAUL R. BROOK,¹² H. THANKFUL CROMARTIE,¹³
KATHRYN CROWTER,¹⁴ MEGAN E. DECESAR,¹⁵ PAUL B. DEMOREST,¹⁶ TIMOTHY DOLCH,^{17,18}
ELIZABETH C. FERRARA,^{19,20,21} WILLIAM FIORE,^{22,23} EMMANUEL FONSECA,^{22,23} GABRIEL E. FREEDMAN,⁸
NATE GARVER-DANIELS,^{22,23} PETER A. GENTILE,^{22,23} JOSEPH GLASER,^{22,23} DEBORAH C. GOOD,²⁴ JEFFREY S. HAZBOUN,²⁵
MARK HUBER,⁵ ROSS J. JENNINGS,^{22,23,*} MEGAN L. JONES,⁸ MATTHEW KERR,²⁶ DUNCAN R. LORIMER,^{22,23} JING LUO,^{27,†}
RYAN S. LYNCH,²⁸ ALEXANDER MCEWEN,⁸ MAURA A. MCLAUGHLIN,^{22,23} NATASHA MCMANN,²⁹ BRADLEY W. MEYERS,^{14,30}
CHERRY NG,³¹ DAVID J. NICE,³² TIMOTHY T. PENNUCCI,³³ BENETGE B. P. PERERA,³⁴ NIHAN S. POL,²⁹
HENRI A. RADOVAN,³⁵ SCOTT M. RANSOM,³⁶ PAUL S. RAY,²⁶ ANN SCHMIEDEKAMP,³⁷ CARL SCHMIEDEKAMP,³⁷
BRENT J. SHAPIRO-ALBERT,^{22,23,38} INGRID H. STAIRS,¹⁴ KEVIN STOVALL,¹⁶ ABHIMANYU SUSOBHANAN,³⁹
JOSEPH K. SWIGGUM,^{32,*} MICHAEL A. TUCKER,^{40,41,‡} AND HALEY M. WAHL^{22,23}

- ¹*Department of Physics and Astronomy, University of Alabama in Huntsville, 301 North Sparkman Drive, Huntsville, AL 35816, USA*
²*SETI Institute, 339 N Bernardo Ave Suite 200, Mountain View, CA 94043, USA*
³*School of Physics and Astronomy, Rochester Institute of Technology, Rochester, NY 14623, USA*
⁴*Laboratory for Multiwavelength Astrophysics, Rochester Institute of Technology, Rochester, NY 14623, USA*
⁵*Institute for Astronomy, University of Hawai'i, 2680 Woodlawn Drive, Honolulu HI 96822*
⁶*Sydney Institute for Astronomy (SIfA), School of Physics, University of Sydney, NSW 2006, Australia*
⁷*Department of Astronomy and Astrophysics, University of California, Santa Cruz, CA 95064, USA*
⁸*Center for Gravitation, Cosmology and Astrophysics, Department of Physics, University of Wisconsin-Milwaukee, P.O. Box 413, Milwaukee, WI 53201, USA*
⁹*Newcastle University, NE1 7RU, UK*
¹⁰*X-Ray Astrophysics Laboratory, NASA Goddard Space Flight Center, Code 662, Greenbelt, MD 20771, USA*
¹¹*Department of Physics and Astronomy, Widener University, One University Place, Chester, PA 19013, USA*
¹²*Institute for Gravitational Wave Astronomy and School of Physics and Astronomy, University of Birmingham, Edgbaston, Birmingham B15 2TT, UK*
¹³*National Research Council Research Associate, National Academy of Sciences, Washington, DC 20001, USA resident at Naval Research Laboratory, Washington, DC 20375, USA*
¹⁴*Department of Physics and Astronomy, University of British Columbia, 6224 Agricultural Road, Vancouver, BC V6T 1Z1, Canada*
¹⁵*George Mason University, Fairfax, VA 22030, resident at the U.S. Naval Research Laboratory, Washington, DC 20375, USA*
¹⁶*National Radio Astronomy Observatory, 1003 Lopezville Rd., Socorro, NM 87801, USA*
¹⁷*Department of Physics, Hillsdale College, 33 E. College Street, Hillsdale, MI 49242, USA*
¹⁸*Eureka Scientific, 2452 Delmer Street, Suite 100, Oakland, CA 94602-3017, USA*
¹⁹*Department of Astronomy, University of Maryland, College Park, MD 20742, USA*
²⁰*Center for Research and Exploration in Space Science and Technology, NASA/GSFC, Greenbelt, MD 20771*
²¹*NASA Goddard Space Flight Center, Greenbelt, MD 20771, USA*
²²*Department of Physics and Astronomy, West Virginia University, P.O. Box 6315, Morgantown, WV 26506, USA*
²³*Center for Gravitational Waves and Cosmology, West Virginia University, Chestnut Ridge Research Building, Morgantown, WV 26505, USA*
²⁴*Department of Physics and Astronomy, University of Montana, 32 Campus Drive, Missoula, MT 59812*
²⁵*Department of Physics, Oregon State University, Corvallis, OR 97331, USA*
²⁶*Space Science Division, Naval Research Laboratory, Washington, DC 20375-5352, USA*
²⁷*Department of Astronomy & Astrophysics, University of Toronto, 50 Saint George Street, Toronto, ON M5S 3H4, Canada*
²⁸*Green Bank Observatory, P.O. Box 2, Green Bank, WV 24944, USA*
²⁹*Department of Physics and Astronomy, Vanderbilt University, 2301 Vanderbilt Place, Nashville, TN 37235, USA*
³⁰*International Centre for Radio Astronomy Research, Curtin University, Bentley, WA 6102, Australia*
³¹*Dunlap Institute for Astronomy and Astrophysics, University of Toronto, 50 St. George St., Toronto, ON M5S 3H4, Canada*

³²*Department of Physics, Lafayette College, Easton, PA 18042, USA*

³³*Institute of Physics and Astronomy, Eötvös Loránd University, Pázmány P. s. 1/A, 1117 Budapest, Hungary*

³⁴*Arecibo Observatory, HC3 Box 53995, Arecibo, PR 00612, USA*

³⁵*Department of Physics, University of Puerto Rico, Mayagüez, PR 00681, USA*

³⁶*National Radio Astronomy Observatory, 520 Edgemont Road, Charlottesville, VA 22903, USA*

³⁷*Department of Physics, Penn State Abington, Abington, PA 19001, USA*

³⁸*Giant Army, 915A 17th Ave, Seattle WA 98122*

³⁹*Max-Planck-Institut für Gravitationsphysik (Albert-Einstein-Institut), Callinstrasse 38, D-30167, Hannover, Germany*

⁴⁰*Center for Cosmology and AstroParticle Physics, 191 W Woodruff Ave, Columbus, OH 43210*

⁴¹*Department of Astronomy, The Ohio State University, 140 W 18th Ave, Columbus, OH 43210*

ABSTRACT

Based on the rate of change of its orbital period, PSR J2043+1711 has a substantial peculiar acceleration of 3.5 ± 0.8 mm/s/yr, which deviates from the acceleration predicted by equilibrium Milky Way models at a 4σ level. The magnitude of the peculiar acceleration is too large to be explained by disequilibrium effects of the Milky Way interacting with orbiting dwarf galaxies (~ 1 mm/s/yr), and too small to be caused by period variations due to the pulsar being a redback. We identify and examine two plausible causes for the anomalous acceleration: a stellar flyby, and a long-period orbital companion. We identify a main-sequence star in *Gaia* DR3 and Pan-STARRS DR2 with the correct mass, distance, and on-sky position to potentially explain the observed peculiar acceleration. However, the star and the pulsar system have substantially different proper motions, indicating that they are not gravitationally bound. However, it is possible that this is an unrelated star that just happens to be located near J2043+1711 along our line of sight (chance probability of 1.6%). Therefore, we also constrain possible orbital parameters for a circumbinary companion in a hierarchical triple system with J2043+1711; the changes in the spindown rate of the pulsar are consistent with an outer object that has an orbital period of 80 kyr, a companion mass of $0.3 M_{\odot}$ (indicative of a white dwarf or low-mass star), and a semi-major axis of 2000 AU. Continued timing and/or future faint optical observations of J2043+1711 may eventually allow us to differentiate between these scenarios.

1. INTRODUCTION

Incredibly precise time-series measurements of pulsars have been pushing the boundaries of astrophysics for several decades. Pulsars have been widely used as tests of strong-field general relativity (Damour & Taylor 1992; Stairs 2003; Antoniadis et al. 2013; Weisberg & Huang 2016), and have recently been used to find the first strong evidence of a gravitational wave background (Agazie et al. 2023a; EPTA Collaboration et al. 2023; Reardon et al. 2023; Xu et al. 2023). The ability to use pulsars as accelerometers is becoming increasingly relevant, and binary millisecond pulsars have already been used to map our Galaxy’s gravitational field without the kinematic assumptions of dynamical equilibrium or symmetry (Chakrabarti et al. 2021; Moran et al. 2023; Donlon et al. 2024). The spin period of solitary millisecond pulsars could in principle also be used if the dependence on the magnetic braking were known, but currently this procedure leads to large uncertainties

(Phillips et al. 2021). The variety of relevant uses for pulsars make them extremely important astrophysical tools; as such, understanding anomalies in the properties of individual pulsars is crucial, as the physics of pulsars can have widespread implications across multiple fields.

PSR J2043+1711 was first discovered by the *Fermi* Large Area Telescope (Atwood et al. 2009; Acero et al. 2015) as a gamma-ray source, and was then shown to be a millisecond pulsar by Guillemot et al. (2012) using the Nançay Radio Telescope. These follow-up observations showed that the pulsar was in a 1.48 day period orbit around a companion, which was likely a helium white dwarf due to its low mass. Due to the pulsar’s particularly stable rotation rate, it was quickly added to the list of pulsars observed by the NANOGrav collaboration, and a measurement of the mass of the pulsar from Shapiro delay was included in the NANOGrav 9-year dataset (NANOGrav Collaboration et al. 2015). The most up-to-date parameters for J2043+1711 use timing data with a 9.2 year baseline from the NANOGrav 15-year data release (Agazie et al. 2023b), where the fit was performed using the ELL1 binary model.

* NANOGrav Physics Frontiers Center Postdoctoral Fellow

† Deceased

‡ CCAPP Fellow

We show that the observed acceleration of J2043+1711, when computed using the parameters provided by the NANOGrav 15-year data release, is statistically inconsistent with predictions from commonly used models for the gravitational potential of the Galaxy. We explore several scenarios that could potentially generate this observed deviation, including dynamical disequilibrium in the Galaxy, a stellar flyby, a circumbinary orbital companion, and J2043+1711 being a spider pulsar. We show that the observed acceleration of J2043+1711 is statistically inconsistent with predictions from commonly used Galactic potential models, because the magnitude of accelerations caused by dynamical disequilibria are too small to explain the observed peculiar acceleration. Similarly, if J2043+1711 were a spider pulsar, it would experience an intrinsic acceleration that is orders of magnitude larger than what we observe for this system. This leaves the stellar flyby and circumbinary companion scenarios as the only two viable options that could explain the observed peculiar acceleration of the system.

Each of these possibilities has distinct ramifications for its respective field: it is now clear that dynamical disequilibrium is essential to understanding our Galaxy, and can be constrained using pulsar timing data (e.g. Antoja et al. 2018; Petersen & Peñarrubia 2021; Donlon et al. 2024); stellar flybys are incredibly rare, and have only been observed a handful of times in young and proto-stellar systems (Dai et al. 2015; Borchert et al. 2022; Cuello et al. 2023); and it is unknown how common circumbinary companions to binary millisecond pulsars are, although at least two such hierarchical triple systems have been shown to exist (Thorsett et al. 1993, 1999; Ransom et al. 2014) and others have been proposed (e.g. Nieder et al. 2022). Additionally, constraining the properties of circumbinary objects could prove useful for understanding the formation processes of pulsar systems. J2043+1711 is a uniquely interesting system that allows us to explore each of these ideas.

This would not be the first time that an unexpected acceleration of a pulsar has led to the discovery of an orbital companion. Matthews et al. (2016) argued that J1024–0719, at the time believed to be an isolated pulsar, had anomalous velocity and acceleration measurements that were consistent with an orbital companion at a large distance from the pulsar. Later, Kaplan et al. (2016) and Bassa et al. (2016) simultaneously showed that J1024–0719 was in a wide orbit around with a K star. While we are unable to determine the cause of the peculiar acceleration for J2043+1711, we hope that the arguments presented in this work will eventually lead to

the confirmation of an additional orbital companion or a stellar flyby.

2. COMPUTING AN ACCELERATION

The NANOGrav 15 year data release incorporated Post-Keplerian orbital parameters such as \dot{P}_b^{Obs} based on a statistical significance F -test that is roughly equivalent to including any such parameter that has significance of $\sim 3\sigma$ or more; see Agazie et al. (2023b) for more details. PSR J2043+1711 was found to have a significant \dot{P}_b^{Obs} using this criterion.

The observed change in the orbital period (\dot{P}_b^{Obs}) of a millisecond pulsar binary system can be decomposed into several independent effects:

$$\dot{P}_b^{\text{Obs}} = \dot{P}_b^{\text{Shk}} + \dot{P}_b^{\text{GR}} + \dot{P}_b^{\text{Int}} + \dot{P}_b^{\Phi}. \quad (1)$$

The term \dot{P}_b^{Shk} is the change in the orbital period (P_b) due to the Shklovskii Effect (Shklovskii 1970), which is caused by transverse motion of the source on the sky leading to an apparent change in the orbital period. The term \dot{P}_b^{GR} is the amount that P_b decreases due to the relativistic decay of the binary orbit from the emission of gravitational waves (Peters & Mathews 1963; Weisberg & Huang 2016), and is a function of the orbital period, eccentricity and masses of the objects in the system. J2043+1711 is not a particularly relativistic system, so in this case \dot{P}_b^{GR} is an order of magnitude smaller than the other terms. Errors were propagated in the standard way for these terms based on individual uncertainties in distance, proper motion, the respective masses, etc.

The term \dot{P}_b^{Int} is a catch-all term for various interactions between a pulsar and its orbital companion. This includes tidal effects, radiative effects, exchanges of mass and/or angular momentum, etc. These effects can be caused either by the strong emission jets radiated by the pulsar interacting with the companion, stellar evolution of the companion causing a change in the configuration of the orbit, or some other complicated process.

The remaining term, \dot{P}_b^{Φ} , corresponds to the amount that P_b changes due to the gravitational potential at the position of the pulsar. The line-of-sight acceleration of the pulsar (relative to the Solar system barycenter) can be calculated as

$$a_{\text{los}} = \mathbf{a} \cdot \hat{\mathbf{x}}_{\text{los}} = \frac{\dot{P}_b^{\Phi}}{P_b} c, \quad (2)$$

where $\hat{\mathbf{x}}_{\text{los}}$ is the unit vector pointing from the Sun to the pulsar. Note that this is not an absolute acceleration with respect to the inertial frame of the Galaxy; rather it is the difference between the potential gradient at the location of the pulsar and the potential gradi-

ent at the Solar position. As such, it is not affected by uncertainties in the Solar location or velocities.

The term \dot{P}_b^Φ is also commonly written as \dot{P}_b^{Gal} , as the relevant quantity is typically the acceleration due to the large-scale gravitational field of the Milky Way (MW), while other effects that can cause accelerations are presumed to be negligible. However, in this case it is helpful to split the line-of-sight acceleration into two distinct components;

$$a_{\text{los}} = a_{\text{los}}^{\text{Gal}} + a_{\text{los}}^{\text{Pec}}, \quad (3)$$

where $a_{\text{los}}^{\text{Gal}}$ is the line-of-sight acceleration due to the large-scale (smooth) gravitational field of the MW, and $a_{\text{los}}^{\text{Pec}}$ is the *peculiar* line-of-sight acceleration of the pulsar due to additional effects.

We are able to calculate a_{los} for PSR J2043+1711 using Equations 1 and 2 with the timing solution from the NANOGrav 15-year data set (Agazie et al. 2023b, see Table 1), yielding $a_{\text{los}} = 2.2 \pm 0.8$ mm/s/yr. Using the MilkyWayPotential2022 model from the **Gala** package (Price-Whelan 2017), we estimate the contribution from the smooth Galactic potential to be $a_{\text{los}}^{\text{Gal}} = -1.47 \pm 0.10$ mm/s/yr, where the uncertainty in this value arises from the uncertainty in the distance to the pulsar. This potential model is fit to observed kinematic data, and therefore represents a reasonable time-static approximation to the true Galactic potential. Using other common kinematic potential models only changes the value of $a_{\text{los}}^{\text{Gal}}$ by a few percent, which does not change the following analysis.

This leads to a peculiar line-of-sight acceleration of $a_{\text{los}}^{\text{Pec}} = 3.7 \pm 0.8$ mm/s/yr. However, Donlon et al. (2024) showed that pulsar accelerations have a global trend relative to kinematic MW models; this effect might be related to dynamical disequilibrium features or a peculiar Solar acceleration, but cannot be explained by processes intrinsic to pulsar timing, and as a result contributes a bias to measured accelerations. The amount of bias expected at the position of J2043+1711 is 0.5 ± 0.1 mm/s/yr, which was determined using the procedure in Section III of Donlon et al. (2024) (see Appendix A for more information on how this calculation is done). Subtracting this amount to remove the bias reduces the peculiar line-of-sight acceleration to $a_{\text{los}}^{\text{Pec}} = 3.2 \pm 0.8$ mm/s/yr. This is roughly double the strength of the expected Galactic acceleration, and represents a 4σ deviation from the underlying Galactic potential models. The possible causes for this peculiar acceleration are explored in the following sections.

Note that we report symmetrical uncertainties throughout this work, although this may not be the case for individual quantities – for example, distance has

PSR J2043+1711	
<i>Fit Parameters</i>	
Spin Frequency Epoch	MJD 57413.000000000
Binary Epoch	TASC = MJD 57413.501338113(3)
f	420.18944316950783(10) s ⁻¹
$f^{(1)}$	-9.25932(2)E-16 s ⁻²
$f^{(2)*}$	3.5(24)E-27 s ⁻³
$f^{(3)*}$	5.8(27)E-34 s ⁻⁴
P_b	1.482290786388(6) days
\dot{P}_b^{Obs}	1.02(12)E-13 s/s
ϖ	0.64(4) mas
<i>Derived Parameters</i>	
d	1.56(10) kpc
μ_α	-5.703(11) mas yr ⁻¹
μ_δ	-10.841(17) mas yr ⁻¹
e	5.01(8)E-6
M_p	1.62(10) M_\odot
M_c	0.190(7) M_\odot
\dot{P}_b^{Shk}	7.3(5)E-14 s/s
\dot{P}_b^{GR}	-2.86(16)E-15 s/s
<i>Gaia</i> DR3 1811439569904158208	
m_G	17.27
M_G	6.0 ^{+0.3} _{-0.2}
$B_P - R_P$	1.13
μ_α	3.81(7) mas yr ⁻¹
μ_δ	0.13(6) mas yr ⁻¹
ϖ	0.57(7) mas
RUWE	0.93
M_{FLAME}	0.80 ^{+0.04} _{-0.05} M_\odot
g_{PS}	17.912(4)
r_{PS}	17.341(4)
i_{PS}	16.935(3)
z_{PS}	16.850(3)
y_{PS}	16.946(7)
RV*	-4(50) km/s

Table 1. Properties of PSR J2043+1711 and *Gaia* DR3 1811439569904158208. The quantities marked with * are fit separately and are not part of the NANOGrav 15-year data set or *Gaia* DR3 catalog.

an asymmetric uncertainty distribution. Donlon et al. (2024) show in their Figure 2 and related discussion that this treatment is appropriate for most pulsars (including J2043+1711), and produces very similar values and uncertainties for inferred accelerations. We have confirmed that this assumption is appropriate for the various components of \dot{P}_b , which have only slightly non-Gaussian posteriors.

PSR	\dot{P}_b/P_b (1/s)
J2043+1711	7.8E-19
J0024-7204W	-1.5E-15
J1023+0038	-4.3E-15
J1048+2339	-1.2E-14
J1227-4853	-3.5E-14
J1622-0315	2.2E-15
J1717+4308A	9.5E-16
J1723-2837	-6.6E-14
J1803-6707	-3.5E-15
J2039-5617	4.1E-16
J2215+5135	-3.0E-14
J2339-0533	-1.2E-14

Table 2. Fractional change in orbital period over time for J2043+1711 compared to those of redback pulsars.

This process was also carried out for all other pulsars in the Donlon et al. (2024) dataset, but only J2043+1711 was found to have a peculiar acceleration that deviates from the expected Galactic acceleration by more than 3σ . This further suggests that the anomalous acceleration of J2043+1711 is actually due to some process occurring specifically for that pulsar – if this phenomenon was a result of incorrectly calculating accelerations for pulsars in general, then we would expect to see the same type of anomalous accelerations in many pulsars, which is not the case.

3. IS J2043+1711 A SPIDER PULSAR?

The first term in Equation 1 that we wish to consider is \dot{P}_b^{Int} , because it is plausible that what the observed peculiar acceleration is not actually a physical acceleration at all, but a variation in the orbital period of the J2043+1711 system due to some sort of complicated interaction between the bound objects. One common type of system that could experience a large \dot{P}_b^{Int} is a redback pulsar.

Spider pulsars are systems where a star has transferred mass to a neutron star companion, recycling the pulsar (Roberts 2013). If the system is oriented so that the pulsar’s radiation jets point at the donor star, they can ablate material away from the companion, leading to evaporation of the donor star on Gyr timescales. The two major categories of spider pulsars are black widows ($M_c < 0.1 M_\odot$) and redbacks ($M_c > 0.1 M_\odot$); in redbacks, the donor star usually becomes a low-mass but overly-luminous star with an extended size and a seemingly normal spectral type (De Vito et al. 2020).

The orbital period, companion mass, and spin period of the J2043+1711 system can potentially classify

the binary as a redback (Swihart et al. 2022), although J2043+1711 is located in an overlapping region shared by redbacks and millisecond pulsar/white dwarf systems. Spider pulsars can experience intrinsic changes in their orbital periods and often have multiple orbital period derivatives, presumably due to tidal interactions with their extended companion and the evaporated outflow from the donor star; if J2043+1711 is in fact a redback, this could plausibly explain the observed peculiar acceleration of the system without requiring any additional nearby objects.

3.1. Eclipses

One way to determine whether a pulsar is a spider is through eclipses; if a pulsar is eclipsed by its companion, then its radio jets are occulted by the evaporated material, confirming that the system is a spider. J2043+1711 does not have apparent eclipses in the phase-wrapped residual of the NANOGrav 15-year dataset. This does not positively rule out the case that J2043+1711 is a redback, as there are many non-eclipsing systems that are confirmed to be spiders (i.e. Agazie et al. 2023b, which discusses 3 non-eclipsing spiders); however, it is a point that argues against the redback scenario, as a significant Shapiro delay and an inclination angle of $i \sim 83^\circ$ has been measured for the J2043+1711 system, which makes it likely that we would detect eclipses if the companion was being strongly irradiated. It is worth noting, though, that because the system would be a long-period redback, this would likely mean that any mass loss from the companion would be minimal (due to the large separation between the two objects), leading to smaller eclipses, and a lower chance of multiple orbital period derivatives and/or tidal interaction.

3.2. Higher Order Orbital Frequency Derivatives

Another way of checking whether the system is a redback is searching for nonzero higher orbital frequency derivatives, which are often present in redback systems. We used PINT (Luo et al. 2021) to fit the NG 15-year data for J2043+1711 with up to four orbital frequency derivatives. None of the higher order derivatives were statistically significant ($< 1\sigma$), which is further evidence that J2043+1711 is not a redback pulsar.

3.3. Scale of Inferred Accelerations for Redbacks

While it is not clear whether the system is actually a redback, the question that remains is that whether J2043+1711 being a redback could actually lead to the observed peculiar acceleration. To test this, we collected a number of measured \dot{P}_b/P_b for redback pulsars, which are provided in Table 2; these quantities are the frac-

tional change in the orbital period over time, and are related to an observed acceleration by a factor of c .

The data from this table comes from the Australia Telescope National Facility Pulsar Catalogue (Manchester et al. 2005), where we have selected a sample of redback pulsars with the following properties:

1. $P_s < 5$ ms
2. $P_b < 1$ day
3. \dot{P}_b exists, and
4. The orbital companion is a main-sequence star.

Note that for many of these systems, the orbital frequency and several time derivatives of the orbital frequency were fit to the timing data instead of the orbital period; in this case, we report

$$\frac{\dot{P}_b}{P_b} = -\frac{\dot{f}_b}{f_b}, \quad (4)$$

where f_b is the orbital frequency and \dot{f}_b is its first time derivative.

All of the redback pulsars have observed values of \dot{P}_b/P_b that are several orders of magnitude larger than the observed value of \dot{P}_b/P_b for J2043+1711. It is therefore unrealistic that the acceleration of J2043+1711 is the result of the system being a bona-fide redback pulsar, because the accelerations that would be inferred due to the orbital interactions of redbacks are hundreds to thousands of larger than the observed peculiar acceleration of J2043+1711.

3.4. Core Mass–Orbital Period Relation

Finally, redbacks of a given mass have a wide range of companion masses. However, companion masses in pulsar–Helium white dwarf systems tend to follow a narrow trend, which is known as the “core mass–orbital period” relation (Tauris & Savonije 1999; Istrate et al. 2014). If J2043+1711 is really in a bound orbit with a Helium white dwarf, the inferred mass of the companion should lie on this relation. The relations given by (Tauris & Savonije 1999) require an estimate of the chemical composition of the companion (i.e. whether its progenitor was a population I or II star), which we do not have. However, assuming the companion’s progenitor was a population I star and plugging in the orbital period for the J2043+1711 system, we predict a companion mass of $0.201 M_\odot$; for a population II object, the companion mass is predicted to be $0.178 M_\odot$. These values bracket the observed mass of the orbital companion, which is further evidence that the companion of J2043+1711 is

in fact a Helium white dwarf, and the system is not a redback pulsar.

Since the system does not appear to be a redback pulsar, we move forwards with the assumption that $\dot{P}_b^{\text{Int}} = 0$; or, in other words, that the observed peculiar acceleration is in fact an actual acceleration caused by a gravitational effect near J2043+1711.

4. GALACTIC CAUSES

The MW is known to currently be in dynamical disequilibrium. This includes corrugations (Xu et al. 2015), vertical density asymmetries (Widrow et al. 2012), and phase space structures (Antoja et al. 2018) in the Galactic disk (where J2043+1711 is located) that are potentially related to interactions between the MW and orbiting satellite dwarf galaxies. Notably, the acceleration field of the MW as measured using pulsars has been shown to be in substantial disequilibrium (Chakrabarti et al. 2021; Donlon et al. 2024). These disequilibrium features have been shown to either be associated with or strongly dependent on the motions of orbiting satellite dwarf galaxies (e.g. Gómez et al. 2017; Antoja et al. 2018). As such, it is plausible that the observed peculiar acceleration of J2043+1711 might be due to some disequilibrium feature in the MW disk that is related to interactions between the MW and its satellite galaxies.

Given a gravitational potential field $\Phi(\mathbf{x})$, the line-of-sight acceleration due to gravity can be calculated as $a_{\text{los}} = -\nabla_{\hat{\mathbf{x}}_{\text{los}}} \Phi(\mathbf{x})$, where $\nabla_{\hat{\mathbf{x}}_{\text{los}}}$ indicates the directional derivative along our line of sight. This allows us to rewrite Equation 3 as a decomposition of the total potential at the location of PSR J2043+1711,

$$\nabla_{\hat{\mathbf{x}}_{\text{los}}} \Phi_{\text{tot}} = \nabla_{\hat{\mathbf{x}}_{\text{los}}} (\Phi_{\text{smooth}} + \Phi_{\text{diseq}}), \quad (5)$$

where Φ_{smooth} is the gravitational potential of the MW if it were in dynamical equilibrium (i.e., its distribution function were static), and Φ_{diseq} is some local perturbation to the static gravitational potential field due to a disequilibrium process. Here, Φ_{smooth} corresponds to $a_{\text{los}}^{\text{Gal}}$ in Equation 3, while Φ_{diseq} corresponds to $a_{\text{los}}^{\text{Pec}}$, although we use different terminology in this case because both Φ_{smooth} and Φ_{diseq} arise from the total gravitational potential of the Galaxy.

Since kinematic models assume dynamical equilibrium, the acceleration predicted by these models corresponds to the acceleration due to Φ_{smooth} . It is unlikely that the observed peculiar acceleration is caused by using an incorrect smooth potential model due to the observed acceleration of J2043+1711 having the opposite sign as the smooth potential model prediction. As a result, in this picture any observed deviation in the acceleration of PSR J2043+1711 must come from Φ_{diseq} .

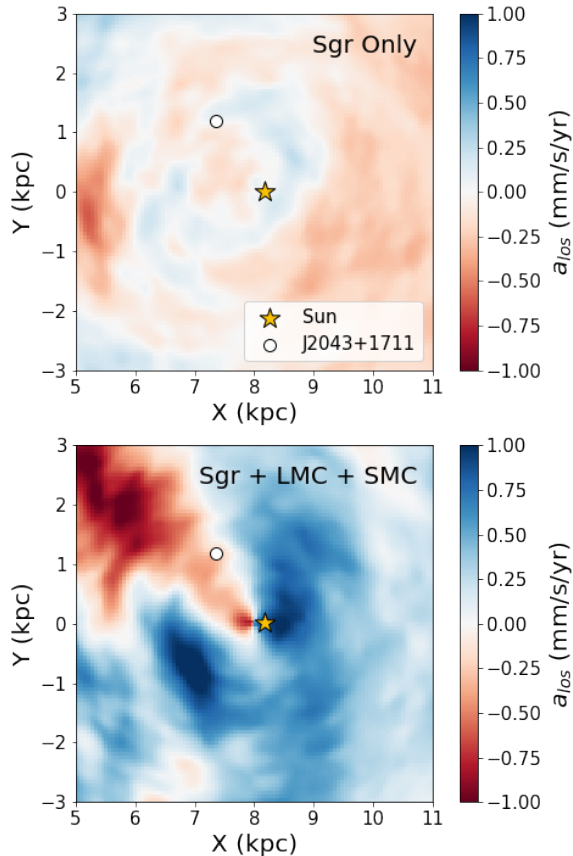


Figure 1. Simulated line-of-sight accelerations that are imparted on the Galactic disk due to interactions with satellite galaxies (Chakrabarti et al. 2019). These accelerations are for objects located in the Galactic plane, i.e. at $Z = 0$. The top panel shows a simulation that only included the effects of the Sgr Dwarf Galaxy, whereas the bottom panel shows the effects of Sgr as well as the Magellanic Clouds. Positive (blue) regions are accelerating away from the Sun, and negative (red) regions are accelerating towards the Sun. These acceleration residuals were obtained by subtracting the accelerations of the initial conditions of the simulation from the accelerations at the present day; this is necessary because the potential of the smooth, unperturbed disk dominates the observed accelerations, and is unrelated to satellite interactions. The typical amplitude of peculiar accelerations due to this particular disequilibrium feature are on the scale of 0.5-1 mm/s/yr, which is not large enough to explain the observed peculiar acceleration for J2043+1711.

Figure 1 shows the peculiar acceleration field that is imparted on the Galactic disk plane in simulations of the Sagittarius Dwarf Galaxy and the Magellanic Clouds interacting with the MW (the details of the simulations are described in Chakrabarti et al. 2019). The large mass of the Magellanic Clouds (e.g. Erkal et al. 2019) and the proximity of the relatively massive Sgr Dwarf Galaxy makes them the main source of external

tidal forces on the MW. The perturbations caused by the satellite interaction are on the order of roughly 1 mm/s/yr near the Sun, which is too small to cause the observed peculiar acceleration of J2043+1711.

These simulated accelerations are also interesting from a Galactic structure perspective. This ~ 1 mm/s/yr perturbation is consistent with the findings of Donlon et al. (2024), who noted that the vertical acceleration profile of the disk is offset by roughly that amount compared to a static equilibrium potential profile. It is worth pointing out that the line-of-sight acceleration at the location of J2043+1711 differs by less than 1 mm/s/yr between most of the disequilibrium potential profiles examined by Donlon et al. (2024) and the static equilibrium potential. Two of the Donlon et al. (2024) models (“local expansion” and “ α - β +2 Point Mass”) deviate from the static equilibrium potential by 3 mm/s/yr at the location of J2043+1711; however, if J2043+1711 is removed from the dataset and these models are then fit again to the remaining pulsars, these deviations become less than 1 mm/s/yr. This indicates that J2043+1711 was strongly biasing these fits, and as a result should probably be removed from future analyses of the Galactic acceleration field.

While the actual masses of the dwarf galaxies could be larger than what was used in these simulations, which would increase the magnitude of the perturbations to the MW disk, it is unlikely that the perturbations from the dwarf in reality are an order of magnitude larger than in this simulation, which would be required to explain J2043+1711’s observed peculiar acceleration.

The presence of disequilibrium effects could reduce the significance of the peculiar acceleration on a $\sim 1\sigma$ level by altering the potential at the location of J2043+1711 in a way that partially explains the observed peculiar acceleration. However, the perturbation could just as easily work in the other direction, making the peculiar acceleration even less consistent with the effect of the underlying Galactic potential. Currently, published simulated models cannot exactly recover the observed perturbations of the Milky Way disk due to the interactions with orbiting satellites (Bennett & Bovy 2021); therefore, we urge the reader not to read into the exact shape and orientation of the acceleration profiles in Figure 1, but instead to look at the broad patterns and magnitudes of the effects, which are more likely to be representative of actual MW disk structure.

It is also possible that dark matter substructure on \sim kpc scales, such as Λ CDM subhalos (Diemand et al. 2007; Bullock & Boylan-Kolchin 2017) or fuzzy dark matter density fluctuations (Hu et al. 2000; Hui et al. 2017) could be responsible for the anomalous accelera-

tion. However, dark matter substructure and interactions with orbiting satellite galaxies should perturb the entire acceleration field on $\sim\text{kpc}$ scales, not only a small region, and therefore cause similar correlated anomalous accelerations for other pulsars in our sample. Since we do not observe similar peculiar accelerations in any of the 11 other pulsars in the Donlon et al. (2024) dataset that have similar measurement precision as J2043+1711 ($S/N > 1$), we conclude that the peculiar acceleration is almost certainly caused by an effect that is local to J2043+1711.

5. STELLAR FLYBY

In order to determine whether the observed peculiar acceleration could be caused by any known optical objects that are near J2043+1711 on the sky, we queried *Gaia* DR3 (Gaia Collaboration et al. 2022). The closest star on the sky to the J2043+1711 system, designated *Gaia* DR3 1811439569904158208, has an angular separation of $2.4''$ from J2043+1711. Further, the parallax of this star is consistent with the parallax of J2043+1711 within their respective error bars: J2043+1711 has a parallax of 0.64 ± 0.04 mas, and the main sequence star has a parallax of 0.57 ± 0.07 mas after applying the *Gaia* DR3 zero-point correction (Lindegren et al. 2021). We checked the impact of the Lutz-Kelker bias (Lutz & Kelker 1973) as it applies to pulsars (Verbiest et al. 2012; Igoshev et al. 2016), and found it to be irrelevant in this case. While additional uncertainty in parallaxes fit to timing data can be potentially problematic depending on how red noise is handled for the source, it is probably not a major source of error for J2043+1711, which has no detectable red noise and consistent timing parallax values throughout previous NANOGrav data sets (Alam et al. 2020; Agazie et al. 2023b).

The proximity of this star to J2043+1711 makes it a plausible candidate for the source of the anomalous acceleration. However, there is a chance that the main-sequence star is unrelated to the J2043+1711 system, and just happens to be located nearby on the sky due to random chance. To test this, we estimated the odds that, given a random point on the sky, we would expect to observe a star brighter than 18th magnitude within $2.5''$ of the selected location. We collected all objects in *Gaia* DR3 brighter than 18th magnitude in 1 square degree of the sky centered on J2043+1711. Over 1 million Monte-Carlo samples, we observe that a randomly-selected point has a 1.6% chance of being located within $2.5''$ of a $G < 18$ star. This does not imply that the association of the star with J2043+1711

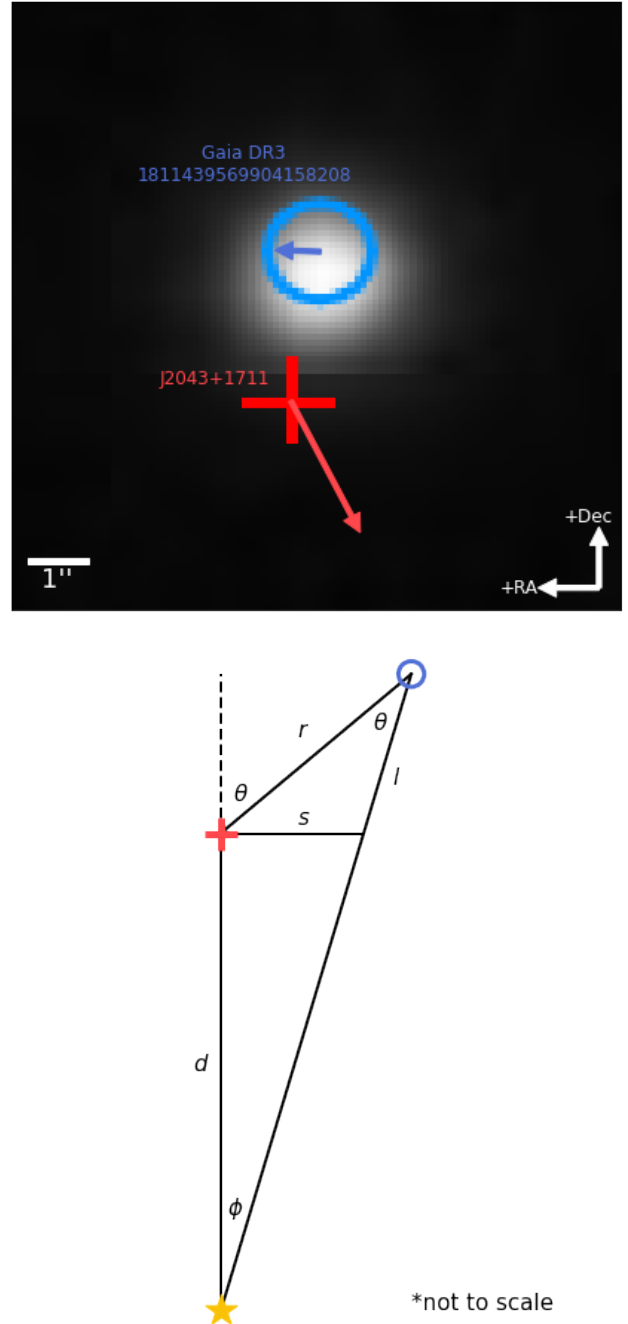


Figure 2. Configuration of J2043+1711 and *Gaia* DR3 1811439569904158208. The top panel shows PS1 photometry; the blue circle shows the location of the main sequence star in *Gaia* DR3, and the red cross is the location of J2043+1711. The arrows show the directions and relative magnitudes of the proper motions of each object. The bottom panel shows a diagram containing the relative distances to each object, as defined in Equation 6. The golden star is the location of the Sun. Note that the two angles labeled θ are equivalent since ϕ is small and $l \ll d$.

is simply due to random chance (especially considering the agreement in the parallaxes of the objects) but it is important to consider that this could still be a specious association.

The mass of the main-sequence star is estimated to be $0.8 M_{\odot}$ based on its photometry using the *Gaia* astrophysical parameter estimation pipeline (Fouesneau et al. 2023). Using this information plus the star’s location on the sky, we can determine the line-of-sight distance between the star and the pulsar that produces the observed peculiar acceleration:

$$a_{\text{los}}^{\text{Pec}} = \frac{GM_{\text{MS}}}{r^2} \cos \theta = \frac{GM_{\text{MS}}\sqrt{r^2 - s^2}}{r^3}, \quad (6)$$

where r is the total distance between the two objects, ϕ is the angle between our line of sight and the vector from the pulsar to the star, $s = d \cos \phi$ is the projected distance between the objects, θ is the angle at J2043+1711 between our line of sight and the main-sequence star, and M_{MS} is the mass of the main sequence star. At a distance of $d = 1.7 \pm 0.1$ kpc (obtained from the weighted mean of the two objects’ parallaxes), $s = 4000 \pm 300$ AU, which sets the line-of-sight distance between the pulsar and the star to be $l = 6500 \pm 700$ AU, and $r = 7700 \pm 700$ AU.

The main-sequence star was also identified in Pan-STARRS DR2 (Chambers et al. 2016), where it has the identifier PSO J310.8369+17.1921. It has a similar apparent magnitude to the *Gaia* observation of the star; the Pan-STARRS photometric data for the star are given in Table 1, and are consistent with the mass and effective temperature listed for this star. This was the closest Pan-STARRS optical source to J2043+1711 on the sky. Another faint object is located $3.2''$ from J2043+1711 in Pan-STARRS, which could potentially be a very low mass star near J2043+1711 given its apparent magnitude $g \sim 25$ and color $g - i \sim 2$. However, this faint object only has 2 detections in Pan-STARRS and fairly large photometric uncertainties, so it is unclear whether it is an actual star; regardless, even if it is a real star located at the optimal line-of-sight distance to maximize an imparted line-of-sight acceleration, its on-sky separation from J2043+1711 and mass of the faint object (based on its color) would not be able to explain the observed peculiar acceleration.

However, J2043+1711 and the *Gaia* main-sequence star do not have similar proper motions, as shown in Table 1. This indicates that if the anomalous acceleration were indeed caused by the gravity of the main sequence star, then J2043+1711 is currently experiencing a stellar flyby.

Renormalized Unit Weight Error, or RUWE, is a measure of how well the *Gaia* astrometric pipeline is able

to fit observations of an object; values above 1.25 indicate that the object is likely a member of a binary due to additional movement on the sky not associated with parallax or proper motion (Penoyre et al. 2022). Our assessment that J2043+1711 and the main-sequence star are not orbiting one another is corroborated by the fact that the RUWE value for the main sequence star in *Gaia* DR3 is only 0.93. Additionally, the *Gaia* DR3 internal classification schema did not identify this star as a likely binary system (Halbwachs et al. 2023). However, it should be noted that at a distance of $r = 7700$ AU, the minimum orbital period of the system is roughly 500,000 years, which is much longer than the ~ 1000 day practical period limit of the *Gaia* DR3 binary classification algorithm (Holl et al. 2023).

5.1. Is *Gaia* DR3 1811439569904158208 a Runaway?

It is possible that the main-sequence star could be a runaway (or hypervelocity) star (Hoogerwerf et al. 2001; Irrgang et al. 2018); these stars are ejected from open clusters or the center of the Galaxy due to close encounters with other stars or the MW’s central black hole, which gives them very large velocities of many hundreds of km/s. This could potentially explain why we observe this object so close to another star, as a runaway would have a velocity very different to that of disk stars. However, the full 3-dimensional velocity of the star is required to determine whether the main-sequence star is actually a runaway.

Using the SuperNova Integral Field Spectrograph (SNIFS, Aldering & Supernova Factory 2007) as part of The Spectroscopic Classification of Astronomical Transients (SCAT, Tucker et al. 2022) Survey, we obtained 2×20 min. $R \sim 1200$ spectra of *Gaia* DR3 1811439569904158208 and a nearby bright *Gaia* standard star (HD197195) with a known line-of-sight velocity of $RV = 29$ km/s (Soubiran et al. 2018); these spectra are shown in Figure 3. Using the Na doublet, $H\alpha$, and 2 of the Ca triplet lines, we measure the line-of-sight velocity of *Gaia* DR3 1811439569904158208 to be $RV = -4$ km/s. Randomly bootstrapping the observed spectra 1000 times using the uncertainty of the flux in each pixel results in an uncertainty of 14 km/s. This is likely an underestimate, as SNIFS has been shown to have a 50 km/s systematic uncertainty when measuring galaxy velocities (Do et al. 2024); however, even with this large uncertainty, the magnitude of the star’s actual line-of-sight velocity should not be much larger than 50 km/s, confidently ruling out a line-of-sight velocity of hundreds of km/s.

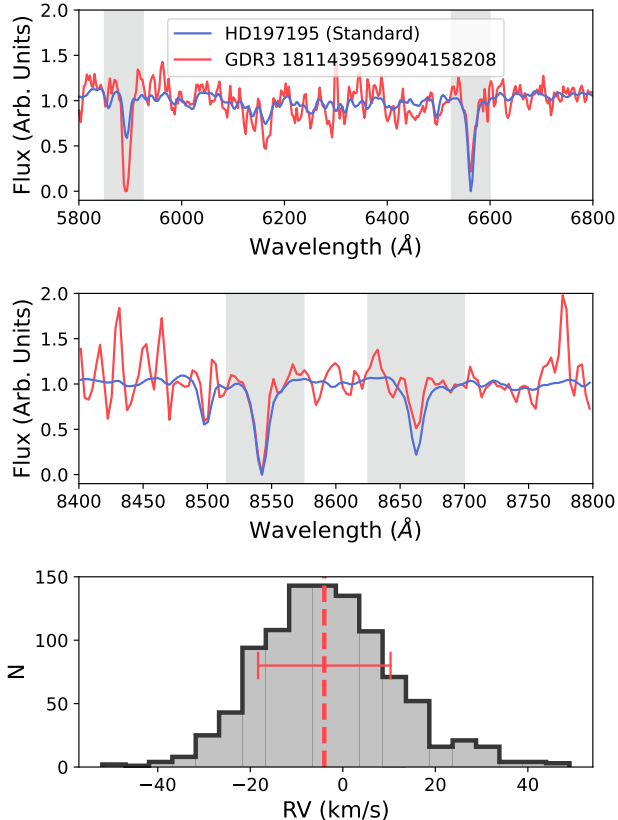


Figure 3. The spectrum and corresponding line-of-sight velocity measurement of *Gaia* DR3 1811439569904158208. $R \sim 1200$ spectra are shown for a standard *Gaia* star with a well-known radial velocity, and *Gaia* DR3 1811439569904158208. The absorption lines that were used to compute line-of-sight velocity are highlighted in gray. The distribution of line-of-sight velocity measurements (after subtracting the velocity of the standard star) from 1000 bootstraps is provided in the bottom panel; it has a median and standard deviation of $RV = -4 \pm 14$ km/s.

Combined with the proper motion of the star, we determine that the star has a 3-dimensional Galactocentric velocity of (11, 224, -16) km/s, total energy of $E \sim -1.25 \times 10^5$ km²/s² and an angular momentum of $L_z \sim -1700$ kpc km/s; these are typical values for a disk star (Deason & Belokurov 2024), indicating that the main-sequence star near J2043+1711 is not a runaway. Varying the line-of-sight velocity of the star within ± 50 km/s does not dramatically change these results.

5.2. Feasibility of a Flyby

As a sanity check, we calculated how far the main sequence star would have traveled relative to J2043+1711 over the 9.2 years that NANOGrav has observed this pulsar. Assuming a relative velocity of 100 km/s (this is slightly larger than the tangential velocity inferred from

the difference in the proper motions of the two objects, and is reasonable, albeit large, for a relative motion between disk objects), the main sequence star would have traveled roughly 200 AU. This is smaller than the uncertainties of the distance between the objects, implying that the variation in line-of-sight acceleration due to the star’s motion over the observation baseline is smaller than the error bars on the observed line-of-sight acceleration. As such, the observed peculiar acceleration is consistent with J2043+1711 experiencing a stellar flyby.

Similarly, we can estimate the probability of a close encounter by assuming that the Galactic midplane has uniform stellar density ρ_* . Then, for any given object, the number of stars within a distance r_0 of that object is

$$N(r < r_0) = \frac{4\pi}{3} \rho_* r_0^3. \quad (7)$$

If we set $\rho_* = 0.0468 M_\odot/\text{pc}^3$ (Guo et al. 2020), each object is expected to have $2.2 \times 10^{-5} M_\odot$ worth of stars within $r_0 = 10,000$ AU. Assuming each star is roughly 1 solar mass, we would expect to observe 1 star within r_0 if we observed roughly 45,000 pulsars. Considering the Donlon et al. (2024) sample of 26 pulsars, this translates to a 1 in roughly 1750 chance, indicating that it is very unexpected but not outside the realm of possibility that we observe a stellar flyby around at least one of these 26 pulsars. Note that J2043+1711 is located 0.4 kpc below the Galactic midplane, which is roughly the scale height of the thin disk; as a result, the density near J2043+1711 will be about a factor of e lower than the midplane density. Similar reductions in density near other pulsars makes this assessment an overestimate, although the bias is not likely to be severe, because most pulsars are located close to the plane.

6. LONG-PERIOD ORBITAL COMPANION

While a stellar flyby is a compelling explanation for the observed peculiar acceleration of J2043+1711, it is not the only possibility. A circumbinary companion with an orbital period much longer than the NANOGrav observation baseline, i.e. a hierarchical triple, would appear to be a constant acceleration in the timing residuals for J2043+1711. This scenario could possibly cause the observed peculiar acceleration.

Gaia has a limiting magnitude of $G \sim 21$; at a distance of 1.6 kpc, this corresponds to an absolute magnitude of $M_G \sim 10$, and any objects fainter than this would not be present in the *Gaia* DR3 catalog. Pan-STARRS has a lower 98% limiting magnitude of $g_{\text{PS}} \sim 23$, requiring that any unseen object near J2043+1711 must be fainter than $M_{g_{\text{PS}}} \sim 12$. This limits any possible circumbinary companion to a neutron star, white dwarf, low-mass (sub-)stellar object, or a black hole.

6.1. Orbital Constraints

The pulses of a pulsar in a binary orbit will be affected by a Römer delay, which induces a sine wave in the observed times of arrival (TOAs) for that pulsar due to the motion of the pulsar around the common center of mass (Lange et al. 2001). For a circular orbit, this delay is described by

$$\Delta_R = x \sin i \sin \left(\frac{2\pi}{P_c} (t - t_0) + \omega \right), \quad (8)$$

where x is the semi-major axis of the orbit, i is the orbital inclination of the system, P_c is the orbital period of the outer binary, and ω is the phase of the orbit at time t_0 .

If the orbital period is sufficiently long compared to the observation baseline, this effect will appear to be stationary, and can be constrained through variations in the spindown rate of the pulsar (Joshi & Rasio 1997; Jones et al. 2023). The derivatives of Δ_R with respect to time provide the line-of-sight velocity of the pulsar, acceleration, jerk, and so on. Because these quantities are related to the Doppler shift by

$$\frac{f^{(1)}}{f} = -\frac{a}{c}, \quad (9)$$

where we have used the notation $f^{(n)} \equiv d^n f / dt^n$, one can continue taking time derivatives of both sides to obtain formulae for the higher-order spindown derivatives. As ω is effectively a nuisance parameter, these quantities can be evaluated at $t = t_0 = 0$ to obtain the general form for this system of equations (Jones et al. 2023):

$$\frac{f^{(n)}}{f} = \frac{x \sin i}{c} \left(\frac{2\pi}{P_c} \right)^{(n+1)} (-1)^{(n+1)} \cos \left(\omega - \frac{n\pi}{2} \right). \quad (10)$$

Note that the above equation only describes a circular orbit; Jones et al. (2023) point out that this is not necessarily a good assumption, and provide instructions on how to extend this result to eccentric orbits.

Jones et al. (2023) also note that successive spindown derivatives that are actually caused by orbital companions should follow an alternating sign pattern based on this formula, caused by successive derivatives of $\cos \omega$. As the NANOGrav 15-year fit only includes f and $f^{(1)}$, we used the PINT software (Luo et al. 2021) to fit additional spindown derivatives up to $f^{(9)}$ to the J2043+1711 TOAs. The existing parameters from the NANOGrav 15-year release were also allowed to vary in this fit, but the optimal values for these parameters did not noticeably change after the addition of the new spindown derivatives.

At some point long-term variations (corresponding to higher-order spindown derivatives) in the TOAs are expected to become dominated by red noise due to effects such as interstellar space weather and the gravitational wave background (Agazie et al. 2023c). To test this, we used PINT to simulate TOAs for a pulsar with all $f^{(n)} = 0$, white noise on the order of $0.1 \mu\text{s}$ (comparable to the observed noise level for J2043+1711 in Agazie et al. 2023b), and red noise generated from a power law with spectral index $\gamma = -3.5$. Fitting the simulated residuals with only spindown derivatives produced apparently significant values with the same alternating sign pattern as is expected from Equation 10. As a result, it is difficult to claim that the higher order spindown derivatives we measure from J2043+1711 are actually due to a circumbinary companion rather than red noise. However, because the NANOGrav 15-year data set did not show significant red noise in J2043+1711 in the first place, we move forward with the assumption that each $f^{(n)}$ is actually due to an orbital companion.

The system of equations defined by Equation 10 are degenerate between $x \sin i$ and P_c (a given orbital period sets the semi-major axis), so we use the measured peculiar acceleration of the system to provide a further constraint on the orbital parameters of the system in order to break this degeneracy. The line-of-sight acceleration is given as

$$a_{\text{los}}^{\text{Pec}} = \frac{GM_c}{x^2} \sin i \sin(-\omega), \quad (11)$$

where $x = x(P_c, M_c)$ can be determined from Kepler's Third Law.

6.2. Markov Chain Monte Carlo Results

Using these constraints, we set up a Markov Chain Monte Carlo (MCMC) simulation using the **emcee** software (Foreman-Mackey et al. 2013) in order to obtain constraints on the possible orbital parameters for a circumbinary orbital companion. This procedure is similar to that of Kaplan et al. (2016) and Bassa et al. (2016), who used comparable fitting methods to discover an orbiting companion around J1024–0719 based on its peculiar acceleration.

The likelihood function for this simulation is defined as

$$\ln \mathcal{L} \left(a_{\text{los,obs}}^{\text{Pec}}, f^{(n)} | P_c, M_c, i, \omega \right) = \ln \mathcal{L}_a + \ln \mathcal{L}_f, \quad (12)$$

where the log-likelihood for observing a given $a_{\text{los}}^{\text{Pec}}$ is

$$\ln \mathcal{L}_a = -\frac{\left(a_{\text{los,obs}}^{\text{Pec}} - a_{\text{los,model}}^{\text{Pec}} \right)^2}{2\sigma_{a_{\text{los}}^{\text{Pec}}}^2}, \quad (13)$$

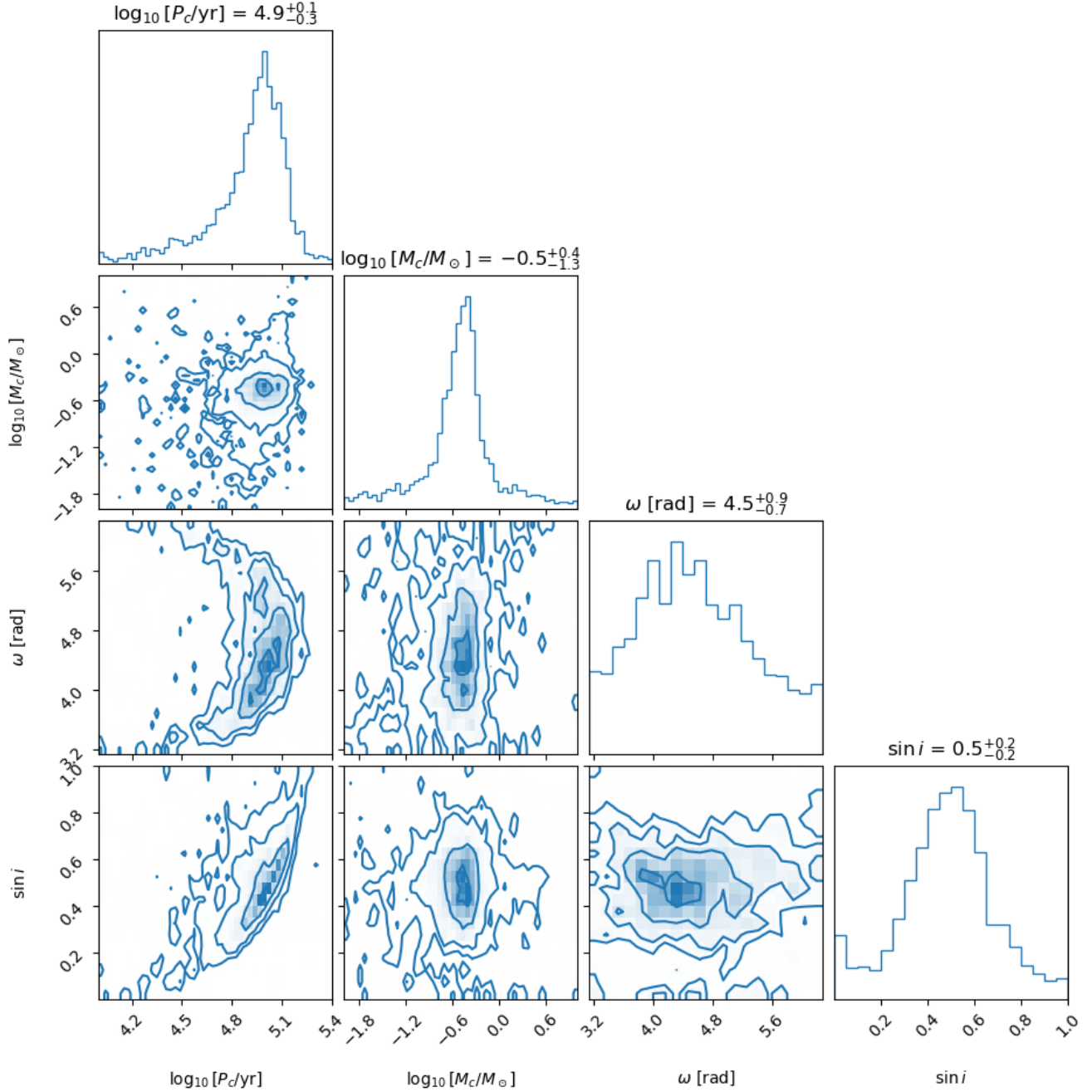


Figure 4. Posterior distributions for orbital parameters of a possible circumbinary companion around J2043+1711. The orbital period and companion mass are well constrained by the model, and the configuration of the orbit is somewhat constrained.

and the likelihood for observing the measured spindown derivatives is

$$\ln \mathcal{L}_f = - \sum_{n=1}^3 \frac{\left(f_{\text{obs}}^{(n)} - f_{\text{model}}^{(n)} \right)^2}{2\sigma_{f^{(n)}}^2}, \quad (14)$$

where $f_{\text{model}}^{(n)}$ and $a_{\text{los,model}}^{\text{Pec}}$ are obtained from Equations 10 and 11, respectively.

Note that only the first three spindown derivatives are used in this setup. This is because higher-order derivatives have progressively larger uncertainties; in order to constrain the four free orbital parameters, we require four constraints, which are provided by three spindown derivatives plus the $a_{\text{los}}^{\text{Pec}}$ constraint. Using all nine spindown derivatives does not substantially change the me-

dian values of the posterior distributions, but it does increase the uncertainties on the reported values.

The results of the MCMC simulation are shown in Figure 4. All orbital parameters are constrained, although the configuration of the orbit is less well constrained than the orbital period and companion mass. The best-fit parameters of the MCMC code produce to an orbit with $P_c = 80$ kyr and $M_c = 0.3 M_\odot$, corresponding to a semi-major axis of $x \approx 2000$ AU. This mass suggests that the companion would probably be a white dwarf or low-mass main sequence star, which would be allowed by the constraints on absolute magnitude given by *Gaia* and PS1 ($M_g \gtrsim 12$). It should be noted that white-dwarf masses below $0.5 M_\odot$ cannot be reached through isolated stellar evolution (i.e. El-Badry et al. 2018); therefore, if this object is a white dwarf, it has likely interacted with at least one other object.

Interestingly, the inclination of the (inner) binary orbit is $\sin i = 0.990$, but the inclination of the possible circumbinary orbit is $\sin i \sim 0.5$. This potentially indicates that the two orbits may not be co-planar, although there is a broad range of posterior values that are consistent with the data, as $\sin i$ is not well constrained.

6.3. Comments on the Orbital Configuration of a Possible Triple System

If J2043+1711 does in fact have a circumbinary companion, this would make it a particularly interesting system for additional study. Pulsar triple systems evolve through complex processes, providing laboratories that test our physical understanding of supernovae and orbital dynamics.

The formation of the inner white dwarf companion to J2043+1711 can be explained through binary evolution where the companion transferred mass onto J2043+1711, recycling the pulsar. The candidate outer companion is likely a low-mass main sequence star given its estimated mass of $0.31_{-0.30}^{+0.48} M_\odot$, although we cannot rule out the candidate companion being a white dwarf. As such, there are several possibilities for the formation of an outer companion, including (but not limited to):

1. The outer companion evolved mostly in isolation. It would be difficult to keep such an object bound to the system after a supernova, although there is some evidence for pulsar formation without large natal kicks (Vigna-Gómez et al. 2018; Willcox et al. 2021).
2. The outer companion evolved elsewhere and was then captured by the inner binary, potentially through an interaction between the inner J2043+1711 system and a second binary system (Mardling & Aarseth 2001).

3. The current outer companion interacted with the pulsar, could potentially undergo mass transfer, and then swapped positions with the current inner white dwarf companion without the triple becoming unstable. This scenario is sensitive to the masses, eccentricity, and inclinations of the orbits in the system, and often leads to a stable configuration where $a_{\text{out}}/a_{\text{in}} \sim 3$ (Mardling & Aarseth 2001), although subsequent supernova kicks could easily change the semi-major axes of the system.
4. Mass loss in the inner binary increased the semi-major axis of the orbit of the outer companion. This could happen either adiabatically or instantaneously through a supernova; the first scenario would imply a low orbital eccentricity for the outer companion, whereas the second scenario implies a large eccentricity (although the eccentricity of the outer system could possibly continue to evolve over time due to other processes).

Particularly relevant for evolved triple systems is the Kozai-Lidov Effect (Shappee & Thompson 2013; Naoz 2016), where interactions between the inner binary and a tertiary companion lead to periodic oscillations in eccentricity and inclination of the inner binary. This allows for the inner binary to reach essentially arbitrarily circular eccentricities ($e \lesssim 10^{-5}$) and could cause tidal interactions or mass transfer in the inner binary, which would potentially explain the current recycled state of J2043+1711. The eccentricity of the inner binary and estimated semi-major axis of ~ 2000 AU ($a_{\text{out}}/a_{\text{in}} \sim 70,000$) for the outer orbit are realistic for this scenario.

It is difficult to make any definitive statement at this point given our relatively weak constraints on the J2043+1711 system. Further complications such as uncertainties in the workings of natal kicks and recycled pulsar formation mechanisms make this a difficult theoretical problem that depends on poorly constrained assumptions. It initially seems unlikely that the outer companion would remain bound to the system, which leads one towards a scenario where the outer companion interacted in some way with the inner binary leading to the present configuration of the system; however, this is speculative, and a series of simulations would be required to understand the relative probabilities of the above scenarios, as well as identifying any other possibilities.

7. DISCUSSION

7.1. Non-trivial Tidal Effects

Since spider pulsars are believed to be a transitional stage of evolution between a classical and millisecond pulsars, one supposes that there may be a phase of the pulsar’s evolution where it is no longer a true redback, but weak evolutionary effects such as mass loss and tidal interactions that could affect the orbital period of the binary system are still present. For example, the companion of J2043+1711 could be a semi-degenerate extended main sequence star, or a Helium white dwarf that still has an extended hydrogen shell.

Classically, tidal effects will cause the orbit to decay, resulting in an observed negative \dot{P}_b (Chakrabarti et al. 2022). This can be calculated as

$$\dot{P}_b^{\text{Tidal}} = -\frac{27\pi}{2} \sum_{i=1,2} \frac{1}{Q'_i} \frac{M_j}{M_i} \left(\frac{R_i}{a}\right)^5, \quad (15)$$

where $j \neq i$, R_i is the radius of each object, M_i is the mass of each object, a is the semimajor axis of the orbit, and Q'_i is the reduced tidal quality factor for an object, which depends on the internal properties and distribution of a body. A rough value of Q'_i for an extended white dwarf is 10^{11} (Fuller & Lai 2013), and Q'_i for a low-mass main sequence star is something like 10^8 (Mathis 2015); a neutron star will be much more rigid than these examples, so we let $1/Q'_i \rightarrow 0$ for the pulsar. Additional tidal terms are typically included to account for \dot{P}_b due to apsidal precession in eccentric orbits; however, this effect is negligible for J2043+1711 given its small eccentricity.

Note that this value is always negative, and the observed \dot{P}_b for J2043+1711 is positive; this indicates that if the observed peculiar acceleration is in-fact due to tidal interactions, they must be complicated. It is clear that the known interactions in redbacks is already more complicated than this simplified picture, as the pulsars in Table 2 have both positive and negative intrinsic accelerations. Because the actual processes at play are unknown, we calculate only the rough order of magnitude for this type of effect below, as the reader should note that the physics of such a phenomenon are not well understood, nor are they handled in a robust way in this work.

In order to obtain the observed change in the orbital period for J2043+1711 ($\dot{P}_b \sim 5.7 \times 10^{-14}$ s/s), Equation 15 requires that a low-mass main sequence star needs a radius of $0.2 R_\odot$, and a white dwarf companion requires a radius of $0.8 R_\odot$. This is an unreasonable radius for a white dwarf, but possible for an extended low-mass main sequence companion. If the companion had this radius and an effective temperature of 4000 K (a typical temperature for a K-M type star, as these extended main sequence companions have normal spectral types

and therefore normal temperatures), then it would have an absolute magnitude of $M_g \sim 9$. This type of objects should have been seen in either the *Gaia* or PS1 catalogs, which we have determined above should see objects as faint as $M_g \sim 11 - 12$ at the distance of J2043+1711. However, it is difficult to know exactly what Q'_i is for an exotic object such as an extended low-mass main sequence star, which could easily change this final result by a magnitude or more. So, while it seems unlikely based on this preliminary analysis that J2043+1711 is experiencing non-trivial tidal interaction effects as it transitions from a bona-fide redback to a non-spider pulsar, we cannot entirely rule out this possibility.

7.2. Negative Dynamical Friction

Massive objects moving through dense space produce an overdense wake behind their direction of motion, which imparts an acceleration antiparallel to the object’s motion vector (Chandrasekhar 1943). This process is known as dynamical friction, and is calculated as

$$a_{\text{DF}} = 0.275 G V_p \sqrt{\frac{\dot{E}}{c} \frac{\rho}{V_w}}, \quad (16)$$

where \dot{E} is the spindown luminosity of the pulsar, ρ is the density of the interstellar medium (ISM, roughly 1 atom per cubic centimeter), V_w is the velocity of the pulsar’s wind emission, and V_p is the velocity of the pulsar relative to the ISM (Gruzinov et al. 2020). For a millisecond pulsar traveling at 75 km/s, this effect is extremely small, roughly 1×10^{-14} mm/s/yr.

The jets emitted by a pulsar carve out a cavity in the ISM, surrounded by an overdense bow shock where the pressure generated by the pulsar emission is equal to the ram pressure of the ISM (e.g. Ramirez-Ruiz et al. 2019). This bow shock is asymmetric, being closest to the pulsar in the direction of the pulsar’s motion. The resulting overdensity in the direction of motion (and lack of nearby material antiparallel to the motion vector) can impart an acceleration onto the pulsar, leading to a negative dynamical friction of the system (Li et al. 2020; Gruzinov et al. 2020). The negative dynamical friction of the system is calculated as

$$a_{\text{NDF}} = 2.31 \frac{G}{V_p} \sqrt{\frac{\dot{E}}{c}} \rho. \quad (17)$$

For a typical millisecond pulsar, $a_{\text{NDF}} \sim 1 \times 10^{-6}$ mm/s/yr. This effect is far too small to be observed in current pulsar acceleration studies. As a result, peculiarities in the bow shock or emission of J2043+1711 cannot cause its observed peculiar acceleration.

Source	Strength ($mm/s/yr$)
Galactic Acceleration	2 – 10
Galactic Disk Disequilibria	0.5 – 1
1 kpc from the LMC ($1.4 \times 10^{11} M_{\odot}$)	9
10 kpc from the LMC	1
60 kpc from the LMC	0.2
2 kpc from a $10^9 M_{\odot}$ dwarf galaxy	4
1 pc from a $10^6 M_{\odot}$ globular cluster	2000
10 pc from a $10^6 M_{\odot}$ globular cluster	50
1 kpc from a $10^8 M_{\odot}$ cold dark matter subhalo	0.5
200 pc from a $10^7 M_{\odot}$ giant molecular cloud	1
5 pc from a $10^4 M_{\odot}$ giant molecular cloud	2
1 pc from a $1 M_{\odot}$ star	0.005
10,000 AU from a $1 M_{\odot}$ star	2
100 AU from a $1 M_{\odot}$ star	20,000
30 AU from a Neptune-mass planet	10
5 AU from a Jupiter-mass planet	7000
1 AU from an Earth-mass planet	600
0.4 AU from a Mercury-mass planet	200
2.5 AU from a 10^{19} kg asteroid	0.0002
Negative dynamical friction	0.000 001
Inferred Redback Pulsar Acceleration	$\gtrsim 10,000$

Table 3. Potential sources of acceleration on objects in the MW, and the approximate strength of each effect.

7.3. Comparing the Strengths of Various Accelerations

There are many different effects that could potentially cause the acceleration of a given object in the Galaxy. These accelerations can point in different directions, and the strength of each effect spans a wide range of orders of magnitude. In Table 3 we provide a list of possible sources of accelerations on objects in the MW, and the approximate magnitude of each effect.

8. CONCLUSIONS

We have shown that the binary millisecond pulsar J2043+1711 has a substantial peculiar acceleration as measured from the rate-of-change of its binary orbital period. The magnitude of the peculiar acceleration is 3.2 ± 0.8 mm/s/yr away from the Sun. The observed acceleration is the opposite sign than the predicted acceleration due to the Galaxy, and is a 4σ deviation from the values predicted by equilibrium Milky Way models.

We show that the magnitude of the peculiar acceleration is too large to be explained by disequilibrium effects of the Milky Way interacting with orbiting dwarf galaxies. While it is possible that this acceleration is caused by (dark matter) substructure in the Galactic density field, it is unlikely that this is the case because we do

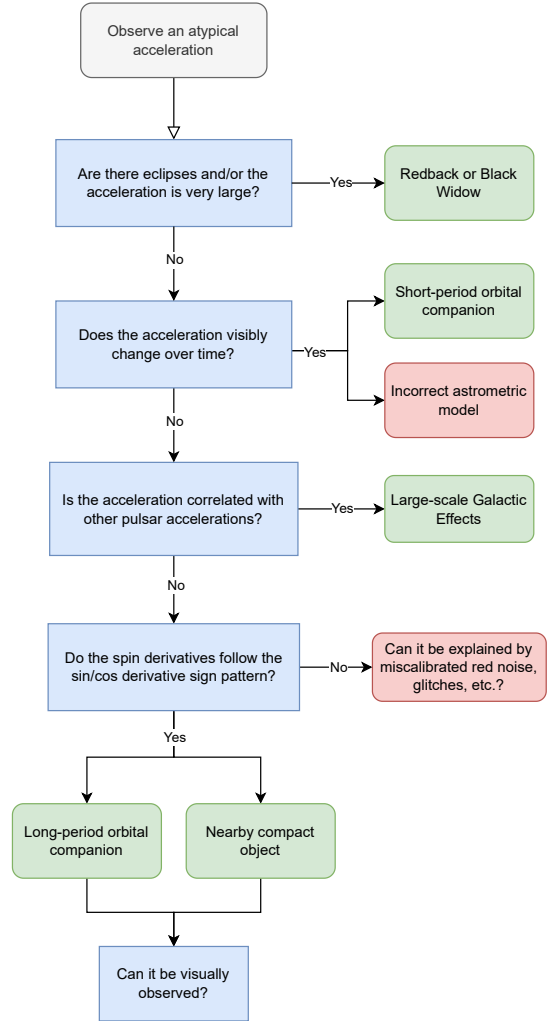


Figure 5. A guide for identifying the cause of anomalous accelerations in pulsars.

not see similar peculiar accelerations in other millisecond binary pulsars.

Similarly, if J2043+1711 were a redback pulsar, this could potentially explain an observed peculiar acceleration. However, the magnitude of intrinsic accelerations generated by redback pulsars are much larger (by several orders of magnitude) than the observed signal for J2043+1711. For this reason, as well as the fact that no eclipses are observed for the system, J2043+1711 has no higher-order orbital period derivatives, and its companion follows the core mass–orbital period relation for Helium white dwarfs, we conclude that the redback scenario cannot be the cause for the observed peculiar acceleration. While J2043+1711 is clearly not a bona-fide

redback, it is possible that the system is in some intermediate stage of evolution between a redback and a typical millisecond pulsar. In this scenario, weak tidal effects from an extended low-mass main sequence star companion could potentially contribute the observed peculiar acceleration; however, this would require that the companion have an absolute magnitude of $M_g \sim 9$, which should have been observed in the *Gaia* and PS1 surveys. We note that the uncertainty on this magnitude could potentially be a magnitude or more, as the tidal quality factor of this type of exotic object is not well known, making it difficult to positively rule out this possibility.

We examine two potential local causes for the anomalous acceleration; a stellar flyby, and a long-period orbital companion. A general outline for identifying the source of an anomalous acceleration is provided in Figure 5, which is followed by this work. Identifying anomalous accelerations will soon become possible with other techniques to measure Galactic accelerations, including in the near future eclipse timing (Chakrabarti et al. 2022), and farther down the road, extreme-precision radial velocity observations (Chakrabarti et al. 2020), where one can expect to follow a similar procedure as outlined in Figure 5 (albeit with different observational schemes).

The star *Gaia* DR3 1811439569904158208 is located close to J2043+1711 both in distance and on-sky position. This main-sequence star has a mass of roughly $0.8 M_\odot$, and could explain the observed peculiar acceleration due to its proximity to J2043+1711. Assuming that this star is the sole cause of the peculiar acceleration, we constrain its line-of-sight distance from J2043+1711 to be 6500 ± 700 AU, and a total distance from the pulsar of 7700 ± 700 AU. However, because the star has a substantially different proper motion than the pulsar, this star cannot be gravitationally bound to J2043+1711; rather, the pulsar would be experiencing a stellar flyby. We obtained spectra for this star and measure the magnitude of its line-of-sight velocity to be $\lesssim 50$ km/s, indicating that it cannot be a runaway (hypervelocity) star.

We fit higher-order spindown derivatives of J2043+1711’s pulse TOAs in order to constrain the properties of a possible circumbinary orbital system. We identify plausible parameters for such a system; the observed properties of J2043+1711 are consistent with the existence of a circumbinary companion that has an orbital period of 80^{+20}_{-40} kyr, a semi-major axis of 2300^{+300}_{-900} AU, and a mass of $0.31^{+0.48}_{-0.30} M_\odot$. Any companion would likely be a white dwarf or low-mass main sequence star due to its mass and the requirement that it be faint enough to not be identified in *Gaia* DR3 or Pan-STARRS DR1.

It is possible that the observed peculiar acceleration is really a combination of multiple effects, i.e., the nearby star plus a circumbinary orbital companion contribute accelerations that when summed together equal the observed peculiar acceleration. It is possible that with future observations of J2043+1711 (which are ongoing with NANOGrav), we might be able to rule out one of these possibilities for the source of the peculiar acceleration. In particular, a longer timing baseline for J2043+1711 will improve uncertainties on higher-order spindown derivatives, which will allow for a higher degree of accuracy when estimating orbital parameters for a candidate circumbinary companion. Alternatively, optical observations down to ~ 26 th magnitude would be able to prove or rule out the existence of a tertiary low-mass stellar or white dwarf companion to the J2043+1711 system.

ACKNOWLEDGMENTS

We would like to thank Alice Quillen and Shami Chatterjee for helpful conversations which improved this work. SC acknowledges support from NSF AAG 2009828 and STSCI GO award 17505.

This paper includes archived data obtained through the Australia Telescope Online Archive (<http://atoa.atnf.csiro.au>).

The NANOGrav Collaboration receives support from the National Science Foundation (NSF) Physics Frontiers Center award No. 2020265. The Arecibo Observatory was a facility of the NSF operated under cooperative agreement (AST-1744119) by the University of Central Florida (UCF) in alliance with Universidad Ana G. Méndez (UAGM) and Yang Enterprises (YEI), Inc.

Portions of this work performed at the U.S. Naval Research Laboratory were supported by ONR 6.1 funding.

The Pan-STARRS1 Surveys (PS1) and the PS1 public science archive have been made possible through contributions by the Institute for Astronomy, the University of Hawaii, the Pan-STARRS Project Office, the Max-Planck Society and its participating institutes, the Max Planck Institute for Astronomy, Heidelberg and the Max Planck Institute for Extraterrestrial Physics, Garching, The Johns Hopkins University, Durham University, the University of Edinburgh, the Queen’s University Belfast, the Harvard-Smithsonian Center for Astrophysics, the Las Cumbres Observatory Global Telescope Network Incorporated, the National Central University of Taiwan, the Space Telescope Science Institute, the National Aeronautics and Space Administration under Grant No. NNX08AR22G issued through the Planetary Science Division of the NASA Science Mission Directorate, the

National Science Foundation Grant No. AST-1238877, the University of Maryland, Eotvos Lorand University (ELTE), the Los Alamos National Laboratory, and the Gordon and Betty Moore Foundation.

Software: Numpy (Harris et al. 2020), Scipy (Virtanen et al. 2020), Sci-kit Learn (Pedregosa et al. 2011), Matplotlib (Hunter 2007), PINT (Luo et al. 2021), Gala (Price-Whelan 2017)

REFERENCES

- Acero, F., Ackermann, M., Ajello, M., et al. 2015, *ApJS*, 218, 23, doi: [10.1088/0067-0049/218/2/23](https://doi.org/10.1088/0067-0049/218/2/23)
- Agazie, G., Anumarlapudi, A., Archibald, A. M., et al. 2023a, *ApJL*, 951, L8, doi: [10.3847/2041-8213/acdac6](https://doi.org/10.3847/2041-8213/acdac6)
- Agazie, G., Alam, M. F., Anumarlapudi, A., et al. 2023b, *ApJL*, 951, L9, doi: [10.3847/2041-8213/acda9a](https://doi.org/10.3847/2041-8213/acda9a)
- Agazie, G., Anumarlapudi, A., Archibald, A. M., et al. 2023c, *ApJL*, 951, L10, doi: [10.3847/2041-8213/acda88](https://doi.org/10.3847/2041-8213/acda88)
- Alam, M. F., Arzoumanian, Z., Baker, P. T., et al. 2020, *The Astrophysical Journal Supplement Series*, 252, 4, doi: [10.3847/1538-4365/abc6a0](https://doi.org/10.3847/1538-4365/abc6a0)
- Aldering, G. S., & Supernova Factory, N. 2007, in *American Astronomical Society Meeting Abstracts*, Vol. 210, American Astronomical Society Meeting Abstracts #210, 82.07
- Antoja, T., Helmi, A., Romero-Gómez, M., et al. 2018, *Nature*, 561, 360, doi: [10.1038/s41586-018-0510-7](https://doi.org/10.1038/s41586-018-0510-7)
- Antoniadis, J., Freire, P. C. C., Wex, N., et al. 2013, *Science*, 340, 448, doi: [10.1126/science.1233232](https://doi.org/10.1126/science.1233232)
- Atwood, W. B., Abdo, A. A., Ackermann, M., et al. 2009, *ApJ*, 697, 1071, doi: [10.1088/0004-637X/697/2/1071](https://doi.org/10.1088/0004-637X/697/2/1071)
- Bassa, C. G., Janssen, G. H., Stappers, B. W., et al. 2016, *MNRAS*, 460, 2207, doi: [10.1093/mnras/stw1134](https://doi.org/10.1093/mnras/stw1134)
- Bennett, M., & Bovy, J. 2021, *MNRAS*, 503, 376, doi: [10.1093/mnras/stab524](https://doi.org/10.1093/mnras/stab524)
- Borchert, E. M. A., Price, D. J., Pinte, C., & Cuello, N. 2022, *MNRAS*, 510, L37, doi: [10.1093/mnrasl/slab123](https://doi.org/10.1093/mnrasl/slab123)
- Bullock, J. S., & Boylan-Kolchin, M. 2017, *ARA&A*, 55, 343, doi: [10.1146/annurev-astro-091916-055313](https://doi.org/10.1146/annurev-astro-091916-055313)
- Chakrabarti, S., Chang, P., Lam, M. T., Vigeland, S. J., & Quillen, A. C. 2021, *ApJL*, 907, L26, doi: [10.3847/2041-8213/abd635](https://doi.org/10.3847/2041-8213/abd635)
- Chakrabarti, S., Chang, P., Price-Whelan, A. M., et al. 2019, *ApJ*, 886, 67, doi: [10.3847/1538-4357/ab4659](https://doi.org/10.3847/1538-4357/ab4659)
- Chakrabarti, S., Stevens, D. J., Wright, J., et al. 2022, *ApJL*, 928, L17, doi: [10.3847/2041-8213/ac5c43](https://doi.org/10.3847/2041-8213/ac5c43)
- Chakrabarti, S., Wright, J., Chang, P., et al. 2020, *ApJL*, 902, L28, doi: [10.3847/2041-8213/abb9b5](https://doi.org/10.3847/2041-8213/abb9b5)
- Chambers, K. C., Magnier, E. A., Metcalfe, N., et al. 2016, *arXiv e-prints*, arXiv:1612.05560, doi: [10.48550/arXiv.1612.05560](https://doi.org/10.48550/arXiv.1612.05560)
- Chandrasekhar, S. 1943, *ApJ*, 97, 255, doi: [10.1086/144517](https://doi.org/10.1086/144517)
- Cuello, N., Ménard, F., & Price, D. J. 2023, *European Physical Journal Plus*, 138, 11, doi: [10.1140/epjp/s13360-022-03602-w](https://doi.org/10.1140/epjp/s13360-022-03602-w)
- Dai, F., Facchini, S., Clarke, C. J., & Haworth, T. J. 2015, *MNRAS*, 449, 1996, doi: [10.1093/mnras/stv403](https://doi.org/10.1093/mnras/stv403)
- Damour, T., & Taylor, J. H. 1992, *PhRvD*, 45, 1840, doi: [10.1103/PhysRevD.45.1840](https://doi.org/10.1103/PhysRevD.45.1840)
- De Vito, M. A., Benvenuto, O. G., & Horvath, J. E. 2020, *MNRAS*, 493, 2171, doi: [10.1093/mnras/staa395](https://doi.org/10.1093/mnras/staa395)
- Deason, A. J., & Belokurov, V. 2024, *arXiv e-prints*, arXiv:2402.12443, doi: [10.48550/arXiv.2402.12443](https://doi.org/10.48550/arXiv.2402.12443)
- Diemand, J., Kuhlen, M., & Madau, P. 2007, *ApJ*, 667, 859, doi: [10.1086/520573](https://doi.org/10.1086/520573)
- Do, A., Shappee, B. J., de Jaeger, T., et al. 2024, *arXiv e-prints*, arXiv:2403.05620, doi: [10.48550/arXiv.2403.05620](https://doi.org/10.48550/arXiv.2403.05620)
- Donlon, Thomas, I., Chakrabarti, S., Widrow, L. M., et al. 2024, *arXiv e-prints*, arXiv:2401.15808, doi: [10.48550/arXiv.2401.15808](https://doi.org/10.48550/arXiv.2401.15808)
- El-Badry, K., Rix, H.-W., & Weisz, D. R. 2018, *ApJL*, 860, L17, doi: [10.3847/2041-8213/aaca9c](https://doi.org/10.3847/2041-8213/aaca9c)
- EPTA Collaboration, InPTA Collaboration, Antoniadis, J., et al. 2023, *A&A*, 678, A50, doi: [10.1051/0004-6361/202346844](https://doi.org/10.1051/0004-6361/202346844)
- Erkal, D., Belokurov, V., Laporte, C. F. P., et al. 2019, *MNRAS*, 487, 2685, doi: [10.1093/mnras/stz1371](https://doi.org/10.1093/mnras/stz1371)
- Foreman-Mackey, D., Hogg, D. W., Lang, D., & Goodman, J. 2013, *PASP*, 125, 306, doi: [10.1086/670067](https://doi.org/10.1086/670067)
- Fouesneau, M., Frémat, Y., Andrae, R., et al. 2023, *A&A*, 674, A28, doi: [10.1051/0004-6361/202243919](https://doi.org/10.1051/0004-6361/202243919)
- Fuller, J., & Lai, D. 2013, *MNRAS*, 430, 274, doi: [10.1093/mnras/sts606](https://doi.org/10.1093/mnras/sts606)
- Gaia Collaboration, Vallenari, A., Brown, A. G. A., et al. 2022, *arXiv e-prints*, arXiv:2208.00211, doi: [10.48550/arXiv.2208.00211](https://doi.org/10.48550/arXiv.2208.00211)
- Gómez, F. A., White, S. D. M., Grand, R. J. J., et al. 2017, *MNRAS*, 465, 3446, doi: [10.1093/mnras/stw2957](https://doi.org/10.1093/mnras/stw2957)
- Gruzinov, A., Levin, Y., & Matzner, C. D. 2020, *MNRAS*, 492, 2755, doi: [10.1093/mnras/staa013](https://doi.org/10.1093/mnras/staa013)
- Guillemot, L., Freire, P. C. C., Cognard, I., et al. 2012, *MNRAS*, 422, 1294, doi: [10.1111/j.1365-2966.2012.20694.x](https://doi.org/10.1111/j.1365-2966.2012.20694.x)
- Guo, R., Liu, C., Mao, S., et al. 2020, *MNRAS*, 495, 4828, doi: [10.1093/mnras/staa1483](https://doi.org/10.1093/mnras/staa1483)
- Halbwachs, J.-L., Pourbaix, D., Arenou, F., et al. 2023, *A&A*, 674, A9, doi: [10.1051/0004-6361/202243969](https://doi.org/10.1051/0004-6361/202243969)
- Harris, C. R., Millman, K. J., van der Walt, S. J., et al. 2020, *Nature*, 585, 357, doi: [10.1038/s41586-020-2649-2](https://doi.org/10.1038/s41586-020-2649-2)
- Holl, B., Sozzetti, A., Sahlmann, J., et al. 2023, *A&A*, 674, A10, doi: [10.1051/0004-6361/202244161](https://doi.org/10.1051/0004-6361/202244161)
- Hoogerwerf, R., de Bruijne, J. H. J., & de Zeeuw, P. T. 2001, *A&A*, 365, 49, doi: [10.1051/0004-6361:20000014](https://doi.org/10.1051/0004-6361:20000014)
- Hu, W., Barkana, R., & Gruzinov, A. 2000, *PhRvL*, 85, 1158, doi: [10.1103/PhysRevLett.85.1158](https://doi.org/10.1103/PhysRevLett.85.1158)
- Hui, L., Ostriker, J. P., Tremaine, S., & Witten, E. 2017, *PhRvD*, 95, 043541, doi: [10.1103/PhysRevD.95.043541](https://doi.org/10.1103/PhysRevD.95.043541)

- Hunter, J. D. 2007, *Computing in Science & Engineering*, 9, 90, doi: [10.1109/MCSE.2007.55](https://doi.org/10.1109/MCSE.2007.55)
- Igoshev, A., Verbunt, F., & Cator, E. 2016, *A&A*, 591, A123, doi: [10.1051/0004-6361/201527471](https://doi.org/10.1051/0004-6361/201527471)
- Irrgang, A., Kreuzer, S., & Heber, U. 2018, *A&A*, 620, A48, doi: [10.1051/0004-6361/201833874](https://doi.org/10.1051/0004-6361/201833874)
- Istrate, A. G., Tauris, T. M., & Langer, N. 2014, *A&A*, 571, A45, doi: [10.1051/0004-6361/201424680](https://doi.org/10.1051/0004-6361/201424680)
- Jones, M. L., Kaplan, D. L., McLaughlin, M. A., & Lorimer, D. R. 2023, *ApJ*, 951, 20, doi: [10.3847/1538-4357/acd248](https://doi.org/10.3847/1538-4357/acd248)
- Joshi, K. J., & Rasio, F. A. 1997, *ApJ*, 479, 948, doi: [10.1086/303916](https://doi.org/10.1086/303916)
- Kaplan, D. L., Kupfer, T., Nice, D. J., et al. 2016, *ApJ*, 826, 86, doi: [10.3847/0004-637X/826/1/86](https://doi.org/10.3847/0004-637X/826/1/86)
- Lange, C., Camilo, F., Wex, N., et al. 2001, *MNRAS*, 326, 274, doi: [10.1046/j.1365-8711.2001.04606.x](https://doi.org/10.1046/j.1365-8711.2001.04606.x)
- Li, X., Chang, P., Levin, Y., Matzner, C. D., & Armitage, P. J. 2020, *MNRAS*, 494, 2327, doi: [10.1093/mnras/staa900](https://doi.org/10.1093/mnras/staa900)
- Lindgren, L., Bastian, U., Biermann, M., et al. 2021, *A&A*, 649, A4, doi: [10.1051/0004-6361/202039653](https://doi.org/10.1051/0004-6361/202039653)
- Luo, J., Ransom, S., Demorest, P., et al. 2021, *ApJ*, 911, 45, doi: [10.3847/1538-4357/abe62f](https://doi.org/10.3847/1538-4357/abe62f)
- Lutz, T. E., & Kelker, D. H. 1973, *PASP*, 85, 573, doi: [10.1086/129506](https://doi.org/10.1086/129506)
- Manchester, R. N., Hobbs, G. B., Teoh, A., & Hobbs, M. 2005, *AJ*, 129, 1993, doi: [10.1086/428488](https://doi.org/10.1086/428488)
- Mardling, R. A., & Aarseth, S. J. 2001, *MNRAS*, 321, 398, doi: [10.1046/j.1365-8711.2001.03974.x](https://doi.org/10.1046/j.1365-8711.2001.03974.x)
- Mathis, S. 2015, in *SF2A-2015: Proceedings of the Annual meeting of the French Society of Astronomy and Astrophysics*, 401–405, doi: [10.48550/arXiv.1511.01084](https://doi.org/10.48550/arXiv.1511.01084)
- Matthews, A. M., Nice, D. J., Fonseca, E., et al. 2016, *ApJ*, 818, 92, doi: [10.3847/0004-637X/818/1/92](https://doi.org/10.3847/0004-637X/818/1/92)
- Moran, A., Mingarelli, C. M. F., Van Tilburg, K., & Good, D. 2023, *arXiv e-prints*, arXiv:2306.13137, doi: [10.48550/arXiv.2306.13137](https://doi.org/10.48550/arXiv.2306.13137)
- NANOGrav Collaboration, Arzoumanian, Z., Brazier, A., et al. 2015, *ApJ*, 813, 65, doi: [10.1088/0004-637X/813/1/65](https://doi.org/10.1088/0004-637X/813/1/65)
- Naoz, S. 2016, *ARA&A*, 54, 441, doi: [10.1146/annurev-astro-081915-023315](https://doi.org/10.1146/annurev-astro-081915-023315)
- Nieder, L., Kerr, M., Clark, C. J., et al. 2022, *ApJL*, 931, L3, doi: [10.3847/2041-8213/ac6b35](https://doi.org/10.3847/2041-8213/ac6b35)
- Pedregosa, F., Varoquaux, G., Gramfort, A., et al. 2011, *Journal of machine learning research*, 12, 2825
- Penoyre, Z., Belokurov, V., & Evans, N. W. 2022, *MNRAS*, 513, 2437, doi: [10.1093/mnras/stac959](https://doi.org/10.1093/mnras/stac959)
- Peters, P. C., & Mathews, J. 1963, *Physical Review*, 131, 435, doi: [10.1103/PhysRev.131.435](https://doi.org/10.1103/PhysRev.131.435)
- Petersen, M. S., & Peñarrubia, J. 2021, *Nature Astronomy*, 5, 251, doi: [10.1038/s41550-020-01254-3](https://doi.org/10.1038/s41550-020-01254-3)
- Phillips, D. F., Ravi, A., Ebadi, R., & Walsworth, R. L. 2021, *PhRvL*, 126, 141103, doi: [10.1103/PhysRevLett.126.141103](https://doi.org/10.1103/PhysRevLett.126.141103)
- Price-Whelan, A. M. 2017, *The Journal of Open Source Software*, 2, doi: [10.21105/joss.00388](https://doi.org/10.21105/joss.00388)
- Ramirez-Ruiz, E., Andrews, J. J., & Schröder, S. L. 2019, *ApJL*, 883, L6, doi: [10.3847/2041-8213/ab3f2c](https://doi.org/10.3847/2041-8213/ab3f2c)
- Ransom, S. M., Stairs, I. H., Archibald, A. M., et al. 2014, *Nature*, 505, 520, doi: [10.1038/nature12917](https://doi.org/10.1038/nature12917)
- Reardon, D. J., Zic, A., Shannon, R. M., et al. 2023, *ApJL*, 951, L6, doi: [10.3847/2041-8213/acdd02](https://doi.org/10.3847/2041-8213/acdd02)
- Roberts, M. S. E. 2013, in *Neutron Stars and Pulsars: Challenges and Opportunities after 80 years*, ed. J. van Leeuwen, Vol. 291, 127–132, doi: [10.1017/S174392131202337X](https://doi.org/10.1017/S174392131202337X)
- Shappee, B. J., & Thompson, T. A. 2013, *ApJ*, 766, 64, doi: [10.1088/0004-637X/766/1/64](https://doi.org/10.1088/0004-637X/766/1/64)
- Shklovskii, I. S. 1970, *Soviet Ast.*, 13, 562
- Soubiran, C., Jasniewicz, G., Chemin, L., et al. 2018, *A&A*, 616, A7, doi: [10.1051/0004-6361/201832795](https://doi.org/10.1051/0004-6361/201832795)
- Stairs, I. H. 2003, *Living Reviews in Relativity*, 6, 5, doi: [10.12942/lrr-2003-5](https://doi.org/10.12942/lrr-2003-5)
- Swihart, S. J., Strader, J., Chomiuk, L., et al. 2022, *ApJ*, 941, 199, doi: [10.3847/1538-4357/aca2ac](https://doi.org/10.3847/1538-4357/aca2ac)
- Tauris, T. M., & Savonije, G. J. 1999, *A&A*, 350, 928, doi: [10.48550/arXiv.astro-ph/9909147](https://doi.org/10.48550/arXiv.astro-ph/9909147)
- Thorsett, S. E., Arzoumanian, Z., Camilo, F., & Lyne, A. G. 1999, *ApJ*, 523, 763, doi: [10.1086/307771](https://doi.org/10.1086/307771)
- Thorsett, S. E., Arzoumanian, Z., & Taylor, J. H. 1993, *ApJL*, 412, L33, doi: [10.1086/186933](https://doi.org/10.1086/186933)
- Tucker, M. A., Shappee, B. J., Huber, M. E., et al. 2022, *PASP*, 134, 124502, doi: [10.1088/1538-3873/aca719](https://doi.org/10.1088/1538-3873/aca719)
- Verbiest, J. P. W., Weisberg, J. M., Chael, A. A., Lee, K. J., & Lorimer, D. R. 2012, *ApJ*, 755, 39, doi: [10.1088/0004-637X/755/1/39](https://doi.org/10.1088/0004-637X/755/1/39)
- Vigna-Gómez, A., Neijssel, C. J., Stevenson, S., et al. 2018, *MNRAS*, 481, 4009, doi: [10.1093/mnras/sty2463](https://doi.org/10.1093/mnras/sty2463)
- Virtanen, P., Gommers, R., Oliphant, T. E., et al. 2020, *Nature Methods*, 17, 261, doi: [10.1038/s41592-019-0686-2](https://doi.org/10.1038/s41592-019-0686-2)
- Weisberg, J. M., & Huang, Y. 2016, *ApJ*, 829, 55, doi: [10.3847/0004-637X/829/1/55](https://doi.org/10.3847/0004-637X/829/1/55)
- Widrow, L. M., Gardner, S., Yanny, B., Dodelson, S., & Chen, H.-Y. 2012, *ApJL*, 750, L41, doi: [10.1088/2041-8205/750/2/L41](https://doi.org/10.1088/2041-8205/750/2/L41)
- Willcox, R., Mandel, I., Thrane, E., et al. 2021, *ApJL*, 920, L37, doi: [10.3847/2041-8213/ac2cc8](https://doi.org/10.3847/2041-8213/ac2cc8)

Xu, H., Chen, S., Guo, Y., et al. 2023, *Research in Astronomy and Astrophysics*, 23, 075024,
doi: [10.1088/1674-4527/acdfa5](https://doi.org/10.1088/1674-4527/acdfa5)

Xu, Y., Newberg, H. J., Carlin, J. L., et al. 2015, *ApJ*, 801,
105, doi: [10.1088/0004-637X/801/2/105](https://doi.org/10.1088/0004-637X/801/2/105)

APPENDIX

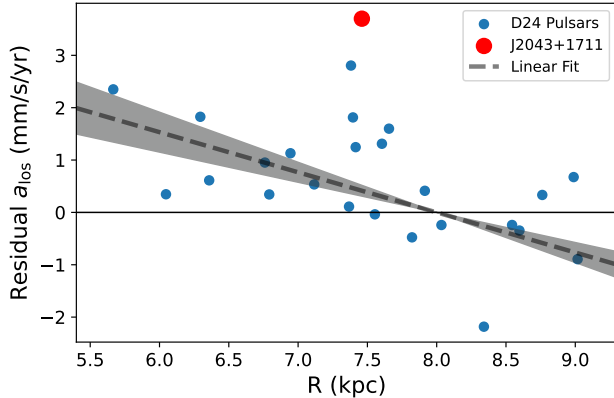


Figure 6. Line-of-sight acceleration bias in pulsars from Donlon et al. (2024), as a function of distance from the center of the Galaxy. J2043+1711 is highlighted as a red point. A linear fit constrained so that it is equal to zero at the Solar location is provided as a dashed line, and the grey region indicates the 1σ error-bars of that value.

A. CALCULATION OF RADIAL ACCELERATION BIAS FOR A GIVEN PULSAR

In Section III of Donlon et al. (2024), it is argued that pulsars near the Sun have biased accelerations. This is shown in their Figure 3, in which they plot a linear fit to the residuals of the line-of-sight accelerations for each pulsar, minus the expected Galactic acceleration for those pulsars. These residuals should be distributed evenly about zero; instead, there is a clear linear trend as a function of their distance from the center of the Galaxy. It is interesting to note that J2043+1711 was not included in this fit, as Donlon et al. (2024) stated that it was an outlier that substantially affected the quality of the linear fit to the residuals.

A reproduction of this fit is provided in Figure 6. We show the acceleration residuals of the D24 pulsars, along with a linear fit to this data. Note that here, we have constrained the linear fit so that it must be equal to zero at the position of the Sun; this was not the case in Donlon et al. (2024), although it is a physically-motivated constraint, and greatly reduces the resulting uncertainty in the linear fit compared to a fit done without this constraint.

The bias $a_{\text{los,B}}$ in the line-of-sight acceleration of any given pulsar can be calculated based on its Galactocentric radius R ,

$$a_{\text{los,B}} = m(R - 8 \text{ kpc}), \quad (\text{A1})$$

where our optimized value for m is -0.77 ± 0.19 mm/s/yr/kpc. At the location of J2043+1711, $R = 7.4$ kpc, leading to an acceleration bias of 0.46 ± 0.11 mm/s/yr.